Chapter 2
Structural and Vibrational Study of Chromyl Fluorosulfate

Abstract In this chapter we present a structural and vibrational study related to chromyl fluorosulfate. The compound was prepared and characterized by infrared spectroscopy. The density functional theory (DFT) has been used to study its structure and vibrational properties. The molecular structure of the compound has been theoretically determined in gas phase employing the B3LYP, B3P86, and B3PW91 levels of theory, and the harmonic vibrational frequencies were evaluated at the same levels. The calculated harmonic vibrational frequencies for chromyl fluorosulfate are consistent with the experimental IR spectrum. These calculations gave us a precise knowledge of the normal modes of vibration taking into account the type of coordination adopted by fluorosulfate groups of this compound as monodentate and bidentate ligands. Also, the assignment of all the observed bands in the IR spectrum for chromyl fluorosulfate was performed. The nature of the Cr–O and Cr ← O bonds and the topological properties of the compound were investigated and analyzed by means of natural bond order (NBO) and *Bader's* Atoms in Molecules theory (AIM), respectively.

Keywords Chromyl fluorosulfate · Vibrational spectra · Molecular structure · Force field · DFT calculations

2.1 Introduction

Since long time, the compounds that contain the V and Cr atoms [1–13] have been studied because many of them present interesting properties, such as the vanadium oxo [2–4, 6, 8, 9, 12] and chromyl compounds [1, 4, 5, 11, 13]. Thus, the chromyl

Adapted from Journal of Molecular Structure,981/1–3, A. Ben Altabef, S.A. Brandán, A New Vibrational Study of Chromyl Fluorosulfate, CrO2 (SO3F)2 by DFT calculations, 146–152, copyright 2010, with permission from Elsevier

DOI: 10.1007/978-94-007-5763-9_2, © The Author(s) 2013

nitrate and perchlorate compounds were theoretical and recently studied by means of the normal mode calculations accomplished by use of a generalized valence force field (GVFF) in order to analyze the coordination modes of the nitrate and perchlorate groups and carry out their complete assignments [11, 13]. These groups can act as monodentate or bidentate ligand [14–19].

The experimental molecular structure of chromyl nitrate has C_2 symmetry [20], while two structures denominate, $C_2(1)$ and $C_2(2)$, were theoretically found for chromyl perchlorate, both with C_2 symmetries [13]. For the $C_2(1)$ structure the two coordination modes are possible, whereas for the $C_2(2)$ structure the perchlorate groups can act only as monodentate ligand. For both molecules, we demonstrate that a molecular force field considering the nitrate and perchlorate groups as monodentate and bidentate ligand calculated using the DFT/B3LYP calculations are well represented [11, 13]. Also, the chromyl fluorosulfate compound, $CrO_2(SO_3F)_2$, presents vibrational properties imperfectly described and only the main characteristics of the infrared spectrum were published in solid phase [21–23].

Initially, this compound was reported by *Lustig* and *Cady* [21] as a dark brown, slightly volatile solid that can be obtained by several methods and it is decomposed at room temperature into a greenish compound. Then, *Rochat* and *Gard* [22] report this compound as a green product relatively stable and nonvolatile at room temperature. When the moss green is heated to 75 °C, it results a stable brown solid. However, the infrared spectra of both solid compounds are the same but; the lines were much sharper and more clearly defined in the brown compound. In this case, we have prepared this compound according to *Brown* and *Gard* [23] and the obtained product was a green solid. The aim of this chapter is to perform an experimental and theoretical study on this compound with the methods of quantum chemistry in order to know its vibrational properties and carry out its complete assignment. In this case, the normal mode calculations were accomplished using a GVFF and considering the fluorosulfate group as monodentate and bidentate ligand. For that purpose, the optimized geometry and frequencies for the normal modes of vibration were calculated. Then, the performed calculations were used to predict the Raman spectrum for which no experimental data exist. For chromyl fluorosulfate, two structures, both with C_2 symmetries, were obtained in similar form to chromyl perchlorate [13]. Bell et al. [24] have found that for chromium, oxo anions and oxyhalide compounds, the B3LYP/Lanl2DZ combination gives the best fit for the geometries and the observed vibrational spectra. In this case, for the two structures of chromyl fluorosulfate, the B3LYP/6-31G* method was used. The force field for both structures of the compound was obtained using the transferable scaling factors of *Rauth* and *Pulay* [25–27] and those scaling factors obtained from chromyl nitrate [11]. Density functional theory (DFT) normal mode assignments, in terms of the potential energy distribution, are in general accord with those obtained from the normal coordinate analysis. In addition, the natural bond order (NBO) [28–31] and atoms in molecules (AIM) [32, 33] calculations were performed in order to study the nature of the two types of Cr–O and Cr ← O bonds and the topological properties of electronic charge density, respectively.

2.2 Structural Study

For chromyl fluorosulfate, using the different methods and basis sets, two different structures were found, as in chromyl perchlorate, both with C_2 symmetries named $C_2(1)$ and $C_2(2)$. In the first structure, the fluorosulfate groups can act as a monodentate or bidentate ligand (Fig. 2.1) while in the second one, the SO_3F^- groups can act only as monodentate ligands (Fig. 2.2).

Table 2.1 shows the comparison of the total energies and dipole moment values for both structures of chromyl fluorosulfate by using the Lanl2dz, STO-3G*, 3-21G*, 6-31G, 6-31G*, 6-311+G, 6-311 ++G, and 6-311 ++G** basis sets with the B3LYP method, while for the B3P86 and B3PW91 methods only the STO-3G* and 6-31G* basis sets were used [34–39].

Note that for the $C_2(1)$ structure, by using the B3LYP method, many basis sets have imaginary frequency values, as also with the B3PW91/6-311G** method, while for the $C_2(2)$ structure all the frequency values were positive. Moreover, the lower energy values for both structures were obtained by using the B3P86/6-311G** combination, while a low energy difference (ΔE) among both structures (0.52 kJ/mol) was obtained by using B3P86/6-31G*, as shown in Table 2.1. A comparison of experimental data for chromyl nitrate with the calculated

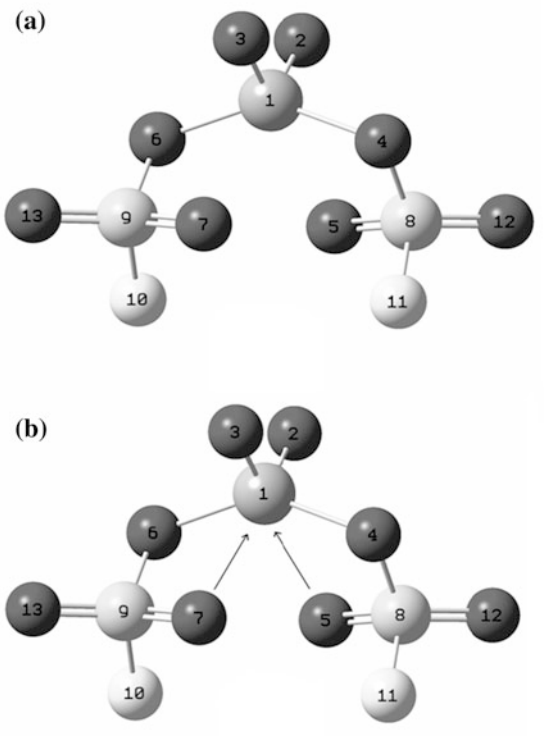

Fig. 2.1 The $C_2(1)$ molecular structure of chromyl fluorosulfate considering the chlorosulfate group as: **a** monodentate ligand and **b** bidentate ligand. Reprinted from Journal of Molecular Structure, 981/1–3, A. Ben Altabef, S.A. Brandán, a new vibrational study of chromyl fluorosulfate, CrO2 (SO3F)2 by DFT calculations 146–152, copyright 2010, with permission from Elsevier

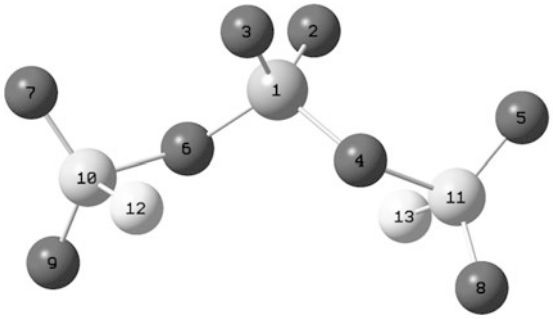

Fig. 2.2 The $C_2(2)$ molecular structure of chromyl fluorosulfate considering the chlorosulfate group as monodentate ligand. Reprinted from Journal of Molecular Structure, 981/1–3, A. Ben Altabef, S.A. Brandán, a new vibrational study of chromyl fluorosulfate, CrO2 (SO3F)2 by DFT calculations 146–152, copyright 2010, with permission from Elsevier

Table 2.1 Total energy (*ET*) and dipole moment () for two structures of chromyl fluorosulfate using different theory levels

B3LYP method						
$C_2(1)$ Symmetry			$C_2(2)$ Symmetry			ΔE
Basis set	*ET* (Hartree)	μ (D)	Basis set	*ET* (Hartree)	μ (D)	kJ/mol
LanL2DZ[a]	−907.5075	1.46	LanL2DZ	−907.5292	1.18	56.92
6-31G[a]	−2641.5519	0.84	6-31G	−2641.5711	0.93	50.36
6-31G*	−2642.1638	0.63	6-31G*	−2642.1671	0.30	8.65
6-31G**	−2642.1638	0.63	6-31G**	−2642.1672	0.30	8.92
6-311G**[a]	−2642.4855	1.48	6-311G**	−2642.4980	1.26	32.78
6-311 + G[a]	−2641.9696	1.62	6-311 + G	−2641.9905	0.07	54.82
6-311 ++G[a]	−2641.9696	1.63	6-311 ++G	−2641.9905	0.07	54.82
6-311 ++G**[a]	−2642.5176	1.40	6-311 ++G**	−2642.5313	1.81	35.93
B3P86 method						
6-31G*	−2644.7194	0.53	6-31G*	−2644.7192	0.29	0.52
6-31G**	−2644.7194	0.53	6-31G**	−2644.7192	0.29	0.52
6-311G**	−2645.0283	1.27	6-311G**	−2645.0354	1.00	18.62
B3PW91 method						
6-31G*	−2641.7296	0.55	6-31G*	−2641.7159	0.57	35.93
6-31G**	−2641.7143	0.58	6-31G**	−2641.7158	0.29	3.93
6-311G**[a]	−2642.0215	1.33	6-311G**	−2642.0303	0.95	23.08

[a] Imaginary frequencies

geometrical parameters for the $C_2(1)$ and $C_2(2)$ structures of chromyl fluorosulfate by using a 6-31G* basis set at different theory levels can be seen in Table 2.2. According to these results, the methods that best reproduce the experimental geometrical parameters for chromyl fluorosulfate with $C_2(1)$ structure is B3PW91/6-31G* where the mean difference for bond lengths is 0.050 Å, while with the B3LYP/6-31G* method it is 5.57° for angles. The functional B3P86 shows a somewhat less satisfactory agreement (5.74°). On the other hand, in the $C_2(2)$

Table 2.2 Comparison of experimental and calculated geometrical parameters at different theory levels for both structures of chromyl fluorosulfate.

$CrO_2(SO_3F)_2$							$CrO_2(NO_3)_2$
Parameter	$C_2(1)$ Symmetry			$C_2(2)$ Symmetry			C_2 Symmetry
	B3LYP 6-31G*	B3PW91	B3P86	B3LYP 6-31G*	B3PW91	B3P86	Ref. [20]
Bond length (Å)							
R(1,2)	1.544	1.541	1.536	1.544	1.536	1.535	1.586 (2)
R(1,3)	1.544	1.541	1.536	1.544	1.536	1.535	1.586 (2)
R(1,4)	1.910	1.913	1.902	1.785	1.778	1.775	1.957 (5)
R(1,5)	2.369	2.315	2.319	3.274	3.264	3.216	2.254 (20)
R(1,6)	1.910	1.913	1.902	1.785	1.778	1.775	1.957 (2)
R(1,7)	2.369	2.315	2.319	3.274	3.264	3.216	2.254 (20)
R(4,8)	1.562	1.551	1.551	1.623	1.614	1.611	
R(5,8)	1.478	1.476	1.474	1.442	1.438	1.437	
R(6,9)	1.562	1.551	1.551	1.623	1.614	1.611	
R(7,9)	1.478	1.476	1.474	1.442	1.438	1.437	
R(8,11)	1.587	1.581	1.577	1.439	1.584	1.581	
R(8,12)	1.436	1.431	1.430	1.439	1.435	1.433	
R(9,10)	1.587	1.581	1.577	1.590	1.584	1.581	
R(9,13)	1.436	1.431	1.430	1.590	1.435	1.433	
RMSD	0.075	0.050	0.057	0.597	0.592	0.566	
Bond angle (°)							
A(2,1,3)	106.7	106.5	106.6	109.1	108.9	108.9	112.2 (71)
A(2,1,4)	103.6	103.4	103.5	110.3	110.3	110.3	97.2 (18)
A(2,1,5)	90.5	90.4	90.5	75.3	75.2	74.5	
A(2,1,6)	97.8	97.2	97.5	107.6	107.6	107.5	104.5 (9)
A(2,1,7)	159.4	159.6	159.6	154.1	153.8	154.7	
A(3,1,4)	97.8	97.2	97.5	107.6	107.6	107.5	104.5 (9)
A(3,1,5)	159.4	159.6	159.6	154.1	153.8	154.7	
A(3,1,6)	103.6	103.4	103.5	110.3	110.3	110.3	97.2 (18)
A(3,1,7)	90.5	90.4	90.5	75.3	75.2	74.5	
A(4,1,5)	66.4	67.2	67.1	49.3	49.2	50.3	
A(4,1,6)	143.7	145.2	144.6	111.8	112.1	112.2	140.5 (9)
A(4,1,7)	84.7	85.1	84.7	91.6	92.1	91.6	
A(5,1,6)	84.7	85.1	84.7	91.6	92.1	91.6	
A(5,1,7)	75.5	75.8	75.4	112.3	112.9	113.6	82.8 (60)
A(6,1,7)	66.4	67.2	67.1	49.3	49.2	50.3	
A(1,4,8)	103.5	101.9	102.5	126.8	126.9	126.1	
A(1,5,8)	87.4	87.9	87.9	68.2	68.1	69.2	
A(1,6,9)	103.5	101.9	102.5	126.8	126.9	126.1	
A(1,7,9)	87.4	87.9	87.9	68.2	68.1	69.2	
A(4,8,5)	102.6	102.7	102.5	109.5	109.6	109.5	
RMSD	5.57	5.90	5.74	13.05	12.96	12.92	

Reprinted from Journal of Molecular Structure, 981/1–3, A. Ben Altabef, S.A. Brandán, a new vibrational study of chromyl fluorosulfate, CrO2 (SO3F)2 by DFT calculations146–152, copyright 2010, with permission from Elsevier

structure, the methods that best reproduce the experimental geometrical parameters for chromyl fluorsulfate is B3P86/6-31G* where the mean difference for bond lengths is 0.566 Å and for angles is 12.92° with the B3PW916-31G* method.

An important observation in the $C_2(2)$ structure is the calculated low value of the O4-Cr1-O6 bond angle with all used methods (between 111.8 and 112.2°) in relation to the experimental value of chromyl nitrate (140.4°). Table 2.3 shows the comparison of the total energies and dipole moment values for fluorosulfate ion with C_{3V} symmetry by using a 6-31G* basis set at different theory levels. Here, the structure with lower energy and dipole moment values by using B3LYP/6-31G* calculation are obtained.

A comparison of the calculated geometrical parameters by using 6-31G* basis set at different theory levels for the fluorosulfate ion to the corresponding experimental values of the SOF_2, SO_2F_2, SO_3 [40], and $LiSO_3F$ [41] compounds in Table 2.4 is shown. These results reveal that the method that best reproduce the

Table 2.3 Total energy (*ET*) and dipole moment () for SO_3F^- ion using 6-31G* basis set at different theory level

Method	*ET* (Hartree)	μ (D)
MP2	−722.3955	0.91
B3PW91	−723.5550	0.85
B3LYP	−723.7217	0.82
B3P86	−724.6294	0.86

Table 2.4 Comparison of experimental and calculated geometrical parameters for SO_3F^- ion using 6-31G* basis set at different theory levels

Parameters	[a]Theoretical					Experimental			
	Ab initio	DFT methods			*Post*HF	[b]SOF_2	[b]SO_2F_2	[b]SO_3	[c]$LiSO_3F$
	HF	B3LYP	B3PW91	B3P86	MP2				
Bond length (Å)									
R(1,2)	1.602	1.670	1.662	1.658	1.667	1.585	1.570		1.555 (7)
R(1,3)	1.436	1.473	1.469	1.467	1.471	1.412	1.370	1.430	1.455 (6)
R(1,4)	1.436	1.473	1.469	1.467	1.471			1.430	1.424 (4)
R(1,5)	1.436	1.473	1.469	1.467	1.471			1.430	1.424 (4)
Bond angle (°)									
A(2,1,3)	102.4	102.1	102.1	102.1	101.9			120	104.5 (5)
A(2,1,4)	102.4	102.1	102.1	102.1	101.9			120	102.8 (3)
A(2,1,5)	102.4	102.1	102.1	102.1	101.9			120	
A(3,1,4)	115.5	115.7	115.7	115.7	115.8				117.4 (4)
A(3,1,5)	115.5	115.7	115.7	115.7	115.8				113.5 (2)
A(4,1,5)	115.5	115.7	115.7	115.7	115.8				

[a] This work
[b] Ref. [40]
[c] Ref. [41]

experimental distances for fluorosulfate ion is HF where the mean difference for bond lengths is 0.014 Å (related to SOF_2), 0.036 Å (related to SO_2F_2), and 0.073 Å (related to $LiSO_3F$). This greater variation in the distance in $LiSO_3F$ is justified, because the SO_3F^- group forms a slightly distorted tetrahedron with a fixed position for the F atom and the S–F in other direction. On the order hand, the theoretical bond angles in all cases are closer to the values for the $LiSO_3F$ compound. The calculated S–O and S–F bond lengths for the fluorosulfate groups corresponding to the $C_2(1)$ structure of chromyl fluorosulfate, by using the three studied methods, are those that better reproduce the experimental geometrical parameters of the SO_3F^- group (related to $LiSO_3F$) with a mean difference of 0.052 Å for distances and 5.5° for angles, while these values for the $C_2(2)$ structure are respectively, 0.090 Å and 6.9°.

The bond orders, expressed by Wiberg's indexes, for both structures by using a B3LYP/6-31G* calculation are shown in Table 2.5. In the $C_2(1)$ structure, the chromium atom forms six bonds, two Cr=O bonds (bond order 2.0077), two Cr–O (bond order 0.4844), and two Cr ← O (bond order 0.1196), while with the other methods the values slightly change. For the $C_2(2)$ structure, the Cr atom forms only four bonds (Table 2.5) because the bond order values for the two Cr ← O bonds change at 0.0158. The DFT calculations predict for both structures that the O4-Cr1-O6 angles are higher than the O_2=Cr1=O_3 bond angle in accordance with the results obtained from chromyl nitrate [20] and perchlorate [13]. This contradiction with the Valence-Shell Electron-Pair Repulsion (VSEPR) theory [42, 43] could be explained in a way similar to other compounds by means of molecular orbital (MO) studies by analyzing the delocalized and/or bonding characters of the relevant MO [7, 11, 13]. The intermolecular interactions for the $C_2(1)$ structure have been analyzed by using *Bader's* topological analysis of the charge electron density, $\rho(r)$ using the AIM program [33].

For the characterization of molecular electronic structure it is important to determine the $\rho(r)$ in the bond critical points (BCPs) and the values of the Laplacian at these points.

The analyses of the Cr–O and Cr ← O BCPs for the $C_2(1)$ structure with the B3LYP/6-31G* and B3P86/6-31G* methods are reported and compared with the corresponding bidentate structure for chromyl perchlorate by using a B3P86/6-31G* level in Table 2.6. Here, there are two important observations, in one case, the Cr1 ← O5 and Cr1 ← O7 BCP have the typical properties of the closed-shell interaction ($\rho(r) = 0.04$ a.u., $|\lambda 1|/\lambda 3 < 1$, and $\nabla^2\rho(r) = 0.20$ a.u.) [44] while the other important observation is related to the topological properties of the Cr1-O4 and Cr1−O6 BCPs, since in both cases they are the same. It is important to note that the properties of the Cr–O and Cr ← O BCPs in chromyl perchlorate are slightly higher than the corresponding values of chromyl fluorosulfate. This difference is related principally with the used method because the properties of chromyl fluorosulfate are closer to chromyl perchlorate when the calculation is performed with the B3P86 method. On the other hand, the (3, +1) critical points confirm the two Cr ← O bonds in the $C_2(1)$ structure of chromyl fluorosulfate (Table 2.6). These two ring points reveal that the coordination mode adopted for

Table 2.5 Wiberg index bond matrix for both structures of chromyl fluorosulfate

B3LYP/6-31G* method													
C_2(1) Symmetry													
Atoms	1	2	3	4	5	6	7	8	9	10	11	12	13
1 Cr	0.0000	2.0077	2.0077	0.4844	0.1196	0.4844	0.1196	0.0135	0.0135	0.0078	0.0078	0.0294	0.0294
2 O	2.0077	0.0000	0.2442	0.0814	0.0076	0.0619	0.0406	0.0048	0.0071	0.0011	0.0012	0.0050	0.0066
3 O	2.0077	0.2442	0.0000	0.0619	0.0406	0.0814	0.0076	0.0071	0.0048	0.0012	0.0011	0.0066	0.0050
4 O	0.4844	0.0814	0.0619	0.0000	0.0838	0.0235	0.0046	0.8908	0.0022	0.0012	0.0516	0.0938	0.0014
5 O	0.1196	0.0076	0.0406	0.0838	0.0000	0.0046	0.0034	1.1840	0.0021	0.0009	0.0753	0.1314	0.0008
6 O	0.4844	0.0619	0.0814	0.0235	0.0046	0.0000	0.0838	0.0022	0.8908	0.0516	0.0012	0.0014	0.0938
7 O	0.1196	0.0406	0.0076	0.0046	0.0034	0.0838	0.0000	0.0021	1.1840	0.0753	0.0009	0.0008	0.1314
8 S	0.0135	0.0048	0.0071	0.8908	1.1840	0.0022	0.0021	0.0000	0.0003	0.0005	0.6575	1.4362	0.0005
9 S	0.0135	0.0071	0.0048	0.0022	0.0021	0.8908	1.1840	0.0003	0.0000	0.6575	0.0005	0.0005	1.4362
10 F	0.0078	0.0011	0.0012	0.0012	0.0009	0.0516	0.0753	0.0005	0.6575	0.0000	0.0001	0.0002	0.0949
11 F	0.0078	0.0012	0.0011	0.0516	0.0753	0.0012	0.0009	0.6575	0.0005	0.0001	0.0000	0.0949	0.0002
12 O	0.0294	0.0050	0.0066	0.0938	0.1314	0.0014	0.0008	1.4362	0.0005	0.0002	0.0949	0.0000	0.0001
13 O	0.0294	0.0066	0.0050	0.0014	0.0008	0.0938	0.1314	0.0005	1.4362	0.0949	0.0002	0.0001	0.0000
C_2(2) Symmetry													
2 O	1.8991	0.0000	0.2537	0.0851	0.0101	0.1051	0.0018	0.0103	0.0053	0.0048	0.0096	0.0032	0.0019
3 O	1.8991	0.2537	0.0000	0.1051	0.0018	0.0851	0.0101	0.0053	0.0103	0.0096	0.0048	0.0019	0.0032
4 O	0.6909	0.0851	0.1051	0.0000	0.1153	0.0516	0.0012	0.0994	0.0020	0.0012	0.6796	0.0007	0.0618
5 O	0.0158	0.0101	0.0018	0.1153	0.0000	0.0012	0.0000	0.2108	0.0002	0.0001	1.3882	0.0001	0.1211
6 O	0.6909	0.1051	0.0851	0.0516	0.0012	0.0000	0.1153	0.0020	0.0994	0.6796	0.0012	0.0618	0.0007
7 O	0.0158	0.0018	0.0101	0.0012	0.0000	0.1153	0.0000	0.0002	0.2108	1.3882	0.0001	0.1211	0.0001
8 S	0.0077	0.0048	0.0096	0.0012	0.0001	0.6796	1.3882	0.0001	1.3969	0.0000	0.0000	0.5915	0.0001
9 S	0.0077	0.0096	0.0048	0.6796	1.3882	0.0012	0.0001	1.3969	0.0001	0.0000	0.0000	0.0001	0.5915
10 F	0.0073	0.0032	0.0019	0.0007	0.0001	0.0618	0.1211	0.0000	0.1210	0.5915	0.0001	0.0000	0.0000
11 F	0.0073	0.0019	0.0032	0.0618	0.1211	0.0007	0.0001	0.1210	0.0000	0.0001	0.5915	0.0000	0.0000
12 O	0.0282	0.0103	0.0053	0.0994	0.2108	0.0020	0.0002	0.0000	0.0001	0.0001	1.3969	0.0000	0.1210
13 O	0.0282	0.0053	0.0103	0.0020	0.0002	0.0994	0.2108	0.0001	0.0000	1.3969	0.0001	0.1210	0.0000

Table 2.6 Analysis of Cr ← O bond critical points in the $C_2(2)$ structure of chromyl fluorosulfate and chromyl perchlorate

[a]Chromyl fluorsulfate						
B3LYP/6-31G* method						
$C_2(1)$ Structure coordination bidentate						
Parameter[c]	Cr1-O4	Cr1 ← O5	Cr1-O6	Cr1 ← O7	(3, +1)	(3, +1)
ρ(r)	0.1114	0.0359	0.1114	0.0359	0.0325	0.03256
$\nabla\rho$(r)	0.5236	0.1340	−0.2090	0.1343	0.1311	−0.0328
$\lambda 1$	−0.2095	−0.0375	−0.1900	−0.0374	−0.0309	−0.0309
$\lambda 2$	−0.1910	−0.0315	−0.1900	−0.0314	0.0401	0.0402
$\lambda 3$	0.9241	0.2030	0.9245	0.2031	0.1218	0.1219
$\lvert\lambda 1\rvert/\lambda 3$	0.2267	0.1847	0.2055	0.1841	0.2536	0.2535
B3P86/6-31G* method						
ρ(r)	0.1142	0.0403	0.1142	0.0403	0.0354	0.0354
$\nabla^2\rho$(r)	0.5380	0.1595	0.5359	0.1591	0.1475	0.1474
$\lambda 1$	−0.2150	−0.0438	−0.2156	−0.0439	−0.0343	−0.0343
$\lambda 2$	0.1959	−0.0389	−0.1969	−0.0391	0.0496	0.0495
$\lambda 3$	0.9489	0.2423	0.9484	0.2421	0.1322	0.1321
$\lvert\lambda 1\rvert/\lambda 3$	0.2266	0.1808	0.2273	0.1813	0.2594	0.2596
[b]Chromyl perchlorate						
B3P86 method						
ρ(r)	0.1191	0.0404	0.1191	0.0404	0.0339	0.03390
$\nabla^2\rho$(r)	0.5641	0.1656	0.5647	0.1663	0.1415	0.1415
$\lambda 1$	−0.2295	−0.0442	−0.2292	−0.0442	−0.0316	−0.0316
$\lambda 2$	−0.2066	−0.0422	−0.2063	−0.0418	0.0463	0.0463
$\lambda 3$	1.0003	0.2521	1.0002	0.2522	0.1268	0.1268
$\lvert\lambda 1\rvert/\lambda 3$	0.2294	0.1753	0.2291	0.1752	0.2492	0.2492

[a] This work; [b] Ref. [13]; [c] The quantities are in atomics units

the fluorosulfate groups in that structure is bidentate. On the other hand, for the $C_2(2)$ structure, using the B3LYP/6-31G* and B3P86/6-31G* methods the Cr ← O BCPs were not possible to be seen, and for this the coordination of the fluorosulfate groups in this structure is only possible as monodentate ligands. The characteristic of these Cr–O BCPs with all the methods used can be seen in Table 2.7. Again, the Cr1-O4 and Cr1-O6 BCPs in chromyl perchlorate are slightly higher with the two methods than the corresponding values of chromyl fluorosulfate.

2.3 Vibrational Study

The two structures of chromyl fluorosulfate have C_2 symmetry and 33 active vibrational normal modes in the infrared and Raman spectra (17 A + 16 B). In this chapter, the study was performed taking into account the monodentate and bidentate coordination modes by fluorosulfate groups, because it is impossible to

Table 2.7 Analysis of Cr–O bond critical points in the $C_2(2)$ structures of chromyl fluorosulfate and chromyl perchlorate at different theory levels

$C_2(2)$ Symmetry coordination monodentate				
Parameter[c]	[a]Chromyl fluorosulfate		[b]Chromyl perchlorate	
	Cr1-O4/Cr1-O6			
	B3LYP 6-31G*	B3P86 6-31G*	B3LYP 6-31G*	B3P86 6-31G*
ρ(r)	0.1478	0.1522	0.1532	0.1573
$\nabla^2\rho$(r)	0.7606	0.7915	0.7634	0.7787
$\lambda 1$	−0.2887	−0.2977	−0.3061	−0.3158
$\lambda 2$	−0.2673	−0.2762	−0.2785	−0.2874
$\lambda 3$	1.3167	1.3665	1.3480	1.3819
$\lvert\lambda 1\rvert/\lambda 3$	0.2192	0.2178	0.2271	0.2285

[a] This work
[b] Ref. [13]
[c] The quantities are in atomics units

make a difference between both coordination modes [18] on the grounds of infrared and Raman spectra alone. The observed frequencies and the assignment for chromyl fluorosulfate are given in Table 2.8. Vibrational assignments were made on the basis of the potential energy distributions (PED) in terms of symmetry coordinates and by comparison with molecules that contain similar groups [1, 11, 13, 22, 23, 45–50]. Here, the results obtained are related at B3LYP level with 6-31G* basis set because after scaling, by using this method, a satisfactory agreement is obtained between the calculated and the experimental vibrational frequencies of chromyl fluorosulfate. In general, the theoretical infrared spectrum of the chromyl fluorosulfate for the $C_2(1)$ structure demonstrates slight agreement with the experimental spectrum, As in Fig. 2.3, it is observed that the theoretical infrared spectrum for the $C_2(2)$ structure is slightly different from the experimental ones. It is possible to observe that in all calculations some vibrational modes of different symmetries are mixed among them because the frequencies are approximately the same. Below we discuss the assignment of the most important groups.

2.4 Coordination Monodentate of the Fluorosulfate Groups

2.4.1 $C_2(1)$ and $C_2(2)$ Symmetries

The frequencies, IR and Raman intensities and PED, obtained by B3LYP/6-31G* calculations considering this mode of coordination for both structures appear in Tables 2.9 and 2.10. Here, the covalent bonding of the fluorosulfate group is easily recognized from its infrared spectrum because the symmetry group changes from the point group C_{3V} of the free ion to C_2 of the compound.

Table 2.8 Experimental and calculated frequencies (cm^{-1}), potential energy distribution and assignment for chromyl fluorosulfate.

Experimental						[a]SQM/B3lyp/6-31G*			[a]Assignment		
						$C_2(1)$		$C_2(2)$	$C_2(1)$		$C_2(2)$
Modes	[a]IR	[b]IR	[c]Raman	[d]IR	[e]IR	M	B	M	Monodentate	Bidentate	Monodentate
A symmetry											
1	1329 s	1438 w	1429 s	1420 w	1308 s	1416	1394	1431	ν_a S=O_2 ip	ν_s S=O	ν_a S=O_2 op
2	1178 sh	1215 vs		1195 s, br		1138	1179	1194	ν_s S=O_2 op	ν_a S–O_2 op	ν_s S=O_2 ip
3	1055 sh	1161 s			1098 m	1001	1010	1117	ν_s S–O_2	ν_s S–O_2 ip	ν_a Cr=O
4	1026 s	1020 vs				961	961	920	ν_s Cr=O	ν_s Cr=O	ν_a S–O_2
5	794 m	926 s	850 (109)	810 s		846	850	820	ν_a S–F	ν_a S–F	ν_a S–F
6	666 sh			618 m	633 m	657	679	665	ν_s Cr–O	δSO_2 op	ν_s Cr–O
7	580 sh		560 (10) p?	575 m	562 m	576	562	535	δSO_2 op	ρSO_2 op	ρSO_2 op
8	534 w		555	550 s		516	509	531	τSO_2 ip	Wag SO_2 op	Wag SO_2 op
9	476 sh					470	475	465	Wag SO_2 op	δS–O–F ip	δCrO_2
10			405 (8) dp		422 m	433	445	417	δCrO_2	δCrO_2	δSO_2 ip
11						359	341	365	δS–O–F ip	τwSO_2 ip	τSO_2 op
12					262 s	273	274	251	τSO_2 op	νCr–O	δS–O–F ip
13						212	220	225	ρ CrO_2	ρCrO_2	τw CrO_2 op
14					165 m	147	148	159	δs Cr–O–S	δCrO_2 ip[f]	τw CrO_2 ip
15						133	136	101	τCr–O–S–O ip	νCr–O	δa Cr–O–S
16					96 w	89	93	36	τw CrO_2 ip	$\tau wCrO_2$ ip	τO–Cr–O–S op
17						51	56	16	τO–Cr–O–S ip	τCr–O–S–O ip	τCr–O–S–O op
B symmetry											
18	1233 sh	1374 vs		1350 s	1207 s	1403	1379	1427	ν_a S=O_2 op	ν_a S=O	ν_a S=O_2 ip
19	1209 vs	1245 s	1230 (6) p			1153	1191	1198	ν_s S=O_2 ip	ν_a S–O_2 ip	ν_s S=O_2 op
20	1026 s	1061 s		1050 s, br		978	979	1102	ν_a S–O_2	ν_s S–O_2 op	ν_s Cr=O
21	989 sh	992 s	960 (6) p	955 s,br		944	946	850	ν_a Cr=O	ν_a Cr=O	ν_s S–O_2
22	871 w	948 m		910 s, br	842 m	847	853	831	ν_s S–F	ν_s S–F	ν_s S–F
23	734 m					665	684	690	ν_a Cr–O	δSO_2 ip	ν_a Cr–O

(continued)

Table 2.8 (continued)

Experimental						[a]SQM/B3lyp/6-31G*			[a]Assignment		
						$C_2(1)$		$C_2(2)$	$C_2(1)$		$C_2(2)$
Modes	[a]IR	[b]IR	[c]Raman	[d]IR	[e]IR	M	B	M	Monodentate	Bidentate	Monodentate
24	611 sh				607 m	584	578	567	δSO_2 ip	ρSO_2 ip	τSO_2 ip
25	514 w					512	506	506	ρSO_2 op	Wag SO_2 ip	ρSO_2 ip
26	450[d]			450 m, br	431 m	456	462	448	ρSO_2 ip	δS–O–F op	δSO_2 op
27			391			361	355	370	δS–O–F op	ν Cr–O	Wag CrO_2
28	330[d]			330 m	309 m	336	334	347	Wag SO_2 ip	τSO_2 op	Wag SO_2 ip
29						237	240	233	Wag CrO_2	Wag CrO_2	ρ CrO_2
30					177 sh	195	204	225	τO–Cr–O–S op	τwCrO_2 op	δS–O–F op
31					121 w	123	128	94	τw CrO_2 op	δCrO_2 op[f]	δs Cr–O–S
32						67	74	22	τCr–O–S–O op	τCr–O–S–O op	τO–Cr–O–S ip
33						10	10	11	δa Cr–O–S	ν Cr–O	τCr–O–S–O ip

Abbreviations: ν stretching, $\boldsymbol{\delta}$, deformation, ρ rocking, wag, (γ) wagging, τw torsion, *a* antisymmetric, *s* symmetric, *op* out-of-phase, *ip* in-phase, *M* monodentate, *B* bidentate, *v* very, *s* strong, *m* medium, *w* weak, *sh* shoulder, *br* broad, *p* polarized, *and dp* depolarized

[a] This work

[b] Ref. [22] $CrO_2(SO_3F)_2$

[c] Ref. [47] HSO_3F

[d] Ref. [23] $CrO_2(SO_3F)_2$

[e] Ref. [45] $Cu(SO_3F)_2$

[f] O–Cr–O deformation

Reprinted from Journal of Molecular Structure, 981/1–3, A. Ben Altabef, S.A. Brandán, a new vibrational study of chromyl fluorosulfate, CrO2 (SO3F)2 by DFT calculations 146–152, copyright 2010, with permission from Elsevier

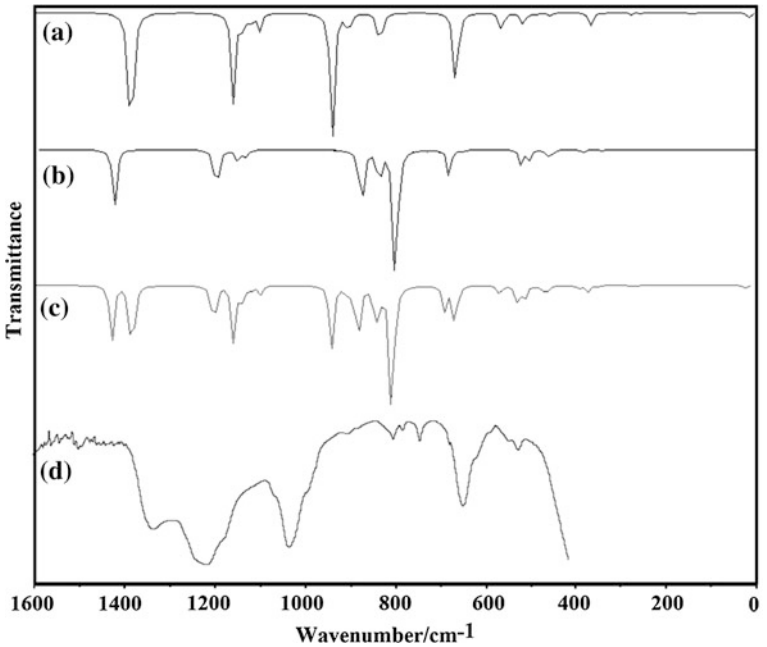

Fig. 2.3 Infrared spectrum of chromyl fluorosulfate: **a** for the theoretical $C_2(1)$ structure; **b** for the $C_2(2)$ theoretical structure; **c** calculated average infrared spectra for both structures from B3LYP/6–31G* wavenumbers and intensities using Lorentzian band shapes (for a population relation $C_2(1)$: $C_2(2)$ of 1: 1 for each structure, and **d** infrared experimental spectrum. Reprinted from Journal of Molecular Structure, 981/1–3, A. Ben Altabef, S.A. Brandán, a new vibrational study of chromyl fluorosulfate, CrO2 (SO3F)2 by DFT calculations146–152, copyright 2010, with permission from Elsevier

2.4.2 Fluorosulfate Groups

The IR bands observed in $CrO_2(SO_3F)_2$ in the 1374–1061 cm^{-1} region were assigned by Rochat and Gard [22] to the two $S{=}O_2$ stretching modes, as in the $Cu(SO_3F)_2$ compound [45] (1308 and 1207 cm^{-1}). In this chapter, the $S{=}O_2$ in-phase and out-of-phase antisymmetric stretching modes for the $C_2(1)$ structure are assigned to the IR band and shoulder at 1329 and 1233 cm^{-1} respectively, while these last two bands, in the $C_2(2)$ structure, are associated with the $S{=}O_2$ out-of-phase and in-phase antisymmetric modes, respectively. The corresponding $S{=}O_2$ out-of-phase and in-phase symmetric stretching modes for the $C_2(1)$ structure are assigned to the very strong band and the shoulder at 1209 and 1178 cm^{-1}, respectively, while in the $C_2(2)$ structure, both bands are associated in an inverse relation with those modes. The SO_2 symmetric and antisymmetric stretching modes are predicted at 1001 and 978 cm^{-1} respectively, for this, these modes in the $C_2(1)$ structure are associated to the shoulder at 1055 cm^{-1} and to the strong band at 1026 cm^{-1}. Experimentally, in the fluorosulfate compounds, the S–F stretching modes are observed between 890 and 700 cm^{-1} [22, 23, 45–50].

Table 2.9 Experimental and calculated frequencies (cm^{-1}), potential energy distribution and assignment for $C_2(1)$ Structure of chromyl fluorosulfate

$C_2(1)$ Structure monodentate coordination

Modes	Observed[a]	Calculated[b]	SQM[c]	PED (≥10 %)
A symmetry				
1	1329 s	1387	1416	ν_a SO_2 ip (75)
2	1178 sh	1127	1138	ν_s SO_2 ip (68) + ν_a SO_2 op (15)
3	1055 sh	1109	1001	ν_s SO_2 (65) + ρ SO_2 op (12)
4	1026 s	931	961	ν_s Cr=O (95)
5	794 m	826	846	ν S–F op (77)
6	666 sh	657	657	wag SO_2 op (34) + ν_s Cr–O (32) + δ Cr–O–S ip (13) + τSO_2 ip (11)
7	580 sh	557	576	τSO_2 ip (47) + δ SO_2 op (23) + ρ SO_2 ip (18)
8	534 w	556	516	τSO_2 ip (44) + δ SO_2 op (14) + τ O–Cr–O–S op (11) + ν S–F op (10)
9	476 sh	478	470	wag SO_2 op (30) + τSO_2 ip (25) + δCrO_2 (23)
10		436	433	δ CrO_2 (40) + wag SO_2 op (17) + τ O–Cr–O–S ip (12)
11		347	359	δ O–S–F ip (37) + δ SO_2 ip (22) + τSO_2 op (20) + τ O–Cr–O–S ip (10)
12		270	273	ν_s Cr–O (31) + τSO_2 op (27) + δ O–S–F ip (11)
13		235	212	ρ CrO_2 (65) + τ O–Cr–O–S ip (12)
14		155	147	δ Cr–O–S ip (36) + ν_s Cr–O (14) + wag SO_2 op (12) + τSO_2 ip (12) + τw CrO_2 ip (12)
15		143	133	τ Cr–O–S–O ip (52) + δ Cr–O–S ip (15) + ρ CrO_2 (14) + τw CrO_2 ip (11)
16		98	89	τ O–Cr–O–S ip (56) + τw CrO_2 ip (31)
17		57	51	τ Cr–O–S–O ip (49) +τ O–Cr–O–S ip (47)
B symmetry				
18	1233 sh	1374	1403	ν_a SO_2 op (76)
19	1209 vs	1149	1153	ν_s SO_2 ip (66) + ν_a SO_2 op (16)
20	1026 s	1091	978	ν_a SO_2 (62) + ν_a Cr=O (20)
21	989 sh	895	944	ν_a Cr=O (70) + ν_a SO_2 (22)
22	871 w	826	847	ν_a S–F (77)

(continued)

Table 2.9 (continued)

$C_2(1)$ Structure monodentate coordination

Modes	Observed[a]	Calculated[b]	SQM[c]	PED (≥10 %)
23	734 m	657	665	ν_a Cr–O (41) + ρ SO_2 ip (22) + τSO_2 ip (18)
24	611 sh	557	584	δSO_2 ip (40) + ρ SO_2 op (27) + wag SO_2 op (10)
25	514 w	506	512	ρ SO_2 op (44) + τSO_2 ip (35)
26	450[d]	449	456	ρ SO_2 ip (49) + τSO_2 ip (15) + δSO_2 op (13)
27		361	361	δ O–S–F op (44) + δSO_2 op (19) + wag CrO_2 (12) + ν_a Cr–O (11)
28	330[d]	336	336	wag SO_2 ip (58) + ν_a Cr–O (11)
29		257	237	wag CrO_2 (68) + δ O–S–F op (14)
30		214	195	τw CrO_2 op (53) + τ O–Cr–O–S op (13)
31		132	123	τw CrO_2 op (29) + δ Cr–O–S op (21) + τ O–Cr–O–S op (14) + τ Cr–O–S–O op (10)
32		75	67	τ Cr–O–S–O op (74) + τw CrO_2 op (12) + τ O–Cr–O–S op (10)
33		10	10	δ Cr–O–S op (25) +τ O–Cr–O–S op (16) + ρ SO_2 ip (15)

[a] This work
[b] DFT B3LYP/6-31G*
[c] From scaled quantum mechanics force field
[d] From Ref. [23]

Table 2.10 Experimental and calculated frequencies (cm^{-1}), potential energy distribution, and assignment for $C_2(2)$ structure of chromyl fluorosulfate

$C_2(2)$ Structure monodentate coordination				
Modes	Observed[a]	Calculated[b]	SQM[c]	PED (≥10 %)
A symmetry				
1	1329 s	1421	1431	ν_a SO_2 ip (57) + ρ SO_2 ip (11) + τSO_2 ip (11)
2	1178 sh	1194	1194	ν_s SO_2 ip (89)
3	1055 sh	1148	1117	ν_a Cr=O (97)
4	1026 s	873	920	ν_a SO_2 (55) + ν_s Cr–O (23) + ρ SO_2 op (11)
5	794 m	797	820	ν S–F op (66) + ν_s SO_2 (13)
6	666 sh	652	665	τSO_2 ip (24) + ν_s Cr–O (21) + ρ SO_2 op (16)
7	580 sh	520	535	ρ SO_2 ip (49) + wag SO_2 op (29)
8	534 w	502	531	wag SO_2 op (32) + ρ SO_2 op (29) + ρ SO_2 ip (22)
9	476 sh	468	465	δCrO_2 (59) + δSO_2 ip (23)
10		420	417	δSO_2 ip (28) + δ CrO_2 (25) + τSO_2 op (14)
11		362	365	τSO_2 op (41) + δSO_2 ip (14) + wagSO_2 ip (12) + τwCrO_2 ip (10) + δO–S–F ip (10)
12		259	251	δ O–S–F ip (55) +ν_s Cr–O (13) + δSO_2 ip (12)
13		232	225	τw CrO_2 op (64)
14		157	159	τw CrO_2 ip (60) + τSO_2 op (10)
15		100	101	δ_a O–S–Cr (61) + τ O–Cr–O–S op (18) + τw CrO_2 op (10)
16		37	36	τ O–Cr–O–S op (61) +δ_a O–S–Cr (15) + τ Cr–O–S–O op (13)
17		17	16	τ Cr–O–S–O op (67) +τ O–Cr–O–S op (17)
B symmetry				
18	1233 sh	1421	1427	ν_a SO_2 ip (65) + ν_a SO_2 op (21)
19	1209 vs	1197	1198	ν_s SO_2 op (87)
20	1026 s	1133	1102	ν_s Cr=O (95)
21	989 sh	837	850	ν_s SO_2 (55) + ν_a Cr–O (33)
22	871 w	831	831	ν_a S–F (54) + τSO_2 ip (16) + ρ SO_2 op (16)
23	734 m	678	690	ν_a Cr–O (35) + ρ SO_2 ip (22) + ν_s SO_2 (19) +ρ SO_2 ip (16)
24	611 sh	521	567	τSO_2 ip (57) + ρ SO_2 ip (32)
25	514 w	501	506	ρ SO_2 ip (62)
26	450[d]	456	448	δSO_2 op (43) + ρ SO_2 ip (20) + wag SO_2 ip (12) + ν_a Cr–O (12)
27		382	370	wag CrO_2 (31) + δ O–S–F op (29) + δSO_2 op (29)
28	330[d]	340	347	wag SO_2 ip (70)
29		232	233	ρCrO_2 (81)
30		224	225	δ O–S–F op (50) + wagCrO_2 (26) + ν_a Cr–O (11)
31		92	94	δs Cr–O–S (86)
32		22	22	τ O–Cr–O–S ip (79) + δs Cr–O–S (10)
33		11	11	δ Cr–O–S ip (58) +τ O–Cr–O–S ip (33)

[a] This work
[b] DFT B3LYP/6-31G*
[c] From scaled quantum mechanics force field
[d] From Ref. [23]

Here, for both structures, those modes are assigned at 871 and 794 cm^{-1}, respectively. For the $C_2(1)$ structure, the SO_2 in-phase and out-of-phase deformation modes are assigned to the shoulders at 611 and 580 cm^{-1} respectively, while these bands in the $C_2(2)$ structure are attributed to the SO_2 in-phase torsion and out-of-phase rocking modes, respectively. The SO_2 wagging, rocking, and twisting modes are observed in the low frequencies region [49, 50]; thus, in the $C_2(1)$ structure, the SO_2 out-of-phase wagging is clearly assigned at 476 cm^{-1}, while the corresponding in-phase mode is assigned, in both structures, at 330 cm^{-1} [23]. For the $C_2(1)$ structure, both rocking modes are calculated with B symmetry and assigned at 514 (out-of-phase) and 450 cm^{-1} (in-phase), while for the other structure these bands are assigned to the in-phase rocking and out-of-phase deformation modes of the SO_2 groups, respectively. The IR band at 450 cm^{-1} is observed in the spectrum obtained by Brown and Gard [23]. The weak band at 534 cm^{-1} is assigned to the SO_2 in-phase twisting mode of the $C_2(1)$ structure while the corresponding out-of-phase mode is associated with the band at 273 cm^{-1}. In the $C_2(2)$ structure, the band at 534 cm^{-1} is assigned to the SO_2 out-of-phase wagging mode while the theoretical band at 251 cm^{-1} is associated with the in-phase S–O–F deformation.

2.4.3 Chromyl Group

In the $C_2(1)$ structure, the Cr=O antisymmetric and symmetric stretchings are split by more than 17 cm^{-1} while that split is of 15 cm^{-1} in the $C_2(2)$ structure, indicating in both cases a slight contribution of the Cr central atom in these vibrations. In the chromyl compounds, these modes appear in the 1,050–900 cm^{-1} region [13, 49, 50]; for this, the intense IR band at 1,026 cm^{-1} is assigned to Cr=O symmetric mode and the shoulder at 989 cm^{-1} is assigned to the corresponding antisymmetric mode of the $C_2(1)$ structure. In the $C_2(2)$ structure, both modes are assigned respectively at 1055 and 1026 cm^{-1}. Despite the fact that the split between both modes is greater in the $C_2(2)$ structure (25 cm^{-1}), both modes are assigned at the same wavenumbers because the O4–Cr1–O6 bond angle is slightly lower in the $C_2(2)$ structure. Thus, for both structures, the band at 734 cm^{-1} and the shoulder at 666 cm^{-1} are associated to these stretching modes, respectively. The CrO_2 bending mode is assigned, as the theoretical calculations predict, at 433 cm^{-1} in the $C_2(1)$ structure, while for the other structure it is assigned to the shoulder located at 476 cm^{-1}. The calculations predict the wagging, rocking, and twisting modes of the CrO_2 group in the low frequencies region and coupled with other modes of the fluorosulfate groups. The assignment of those modes for both structures is different from each other, as observed in Tables 2.9 and 2.10, and moreover both structures are assigned according to the calculations, because it was not possible to observe bands in this region. Thus, for the $C_2(1)$ structure, the wagging CrO_2 mode is calculated at a higher frequency (237 cm^{-1}) than the rocking mode (212 cm^{-1}) while the twisting mode is calculated at 123 cm^{-1}. On

the other hand, in the $C_2(2)$ structure, the rocking mode is calculated (233 cm^{-1}) at lower frequency than the CrO_2 wagging mode (347 cm^{-1}) while the twisting mode is calculated at 159 cm^{-1}.

2.5 Coordination Bidentate of the Fluorosulfate Groups

2.5.1 $C_2(1)$ Symmetry

The observed and calculated IR frequencies and potential energy distribution obtained by B3LYP/6-31G* calculations considering the bidentate coordination appear in Table 2.11.

2.5.2 Fluorosulfate Groups

In this case, there are slight changes in the PED contribution and in the coupling of the modes. Here, the S=O symmetric stretching mode is calculated at higher wavenumbers than the corresponding antisymmetric mode; for this, the strong IR band at 1329 cm^{-1} and the shoulder at 1233 cm^{-1} is assigned, respectively, to these modes. The assignment of the bands associated to the SO_2 out-of-phase and in-phase antisymmetric and symmetric modes is similar to the monodentate type, as shown in Table 2.8, while the SO_2 in-phase and out-of-phase deformation modes are assigned, respectively, to the bands at 734 and 666 cm^{-1}. The SO_2 out-of-phase and in-phase wagging modes are assigned to the weak bands at 534 and 514 cm^{-1}, respectively. Both rocking modes are calculated with different symmetry and assigned to the shoulders at 580 (out-of-phase) and 611 cm^{-1} (in-phase), respectively. Finally, the band at 330 cm^{-1} is associated with SO_2 out-of-phase twisting while the corresponding in-phase mode is assigned according to calculations at 341 cm^{-1}.

2.5.3 Chromyl Group

Here, two Cr=O stretching modes and four Cr–O stretching modes are expected due to bidentate coordination of the fluorosulfate groups (Fig. 1.b). In chromyl compounds, the Cr=O stretching is observed in the 1050–900 cm^{-1} region [4, 12, 13, 47, 50]; for this reason, these modes are easily assigned (Table 2.8). One important observation is that the CrO_2 bending (O=Cr=O) mode appears at the same wavenumbers that in the monodentate case. Hence, it is possible to observe this mode at 445 cm^{-1} (56 %) while in chromyl nitrate it is observed at 475 cm^{-1}

Table 2.11 Experimental and calculated frequencies (cm^{-1}), potential energy distribution and assignment for $C_2(1)$ Structure of chromyl fluorosulfate

$C_2(1)$ Structure bidentate coordination				
Modes	Observed[a]	Calculated[b]	SQM[c]	PED (≥10 %)
A symmetry				
1	1329 s	1387	1394	ν_s S=O (51) + ν_s SO_2 ip (30) + ν_a SO_2 op (10)
2	1178 sh	1127	1179	ν_a SO_2 op (46) + ν_s S=O (38)
3	1055 sh	1109	1010	ν_s SO_2 ip (48) + ν_a SO_2 op (34)
4	1026 s	931	961	ν_s Cr=O (95)
5	794 m	826	850	ν_a S–F (76)
6	666 sh	657	679	δ SO_2 op (42) + ν Cr–O (23)
7	580 sh	557	562	ρ SO_2 op (55) δ O–S–F ip (12) + ν Cr–O (12)
8	534 w	556	509	wag SO_2 op (61) + δ O–S–F ip (17)
9	476 sh	478	475	δO–S–F ip (27) + δCrO_2 (18) + νCr–O (14) + ρSO_2 op (14) + δSO_2 ip (11)
10		436	445	δCrO_2 (56) + δ O–S–F ip (19) + τw CrO_2 ip (13)
11		347	341	τSO_2 ip (80)
12		270	274	δ SO_2 ip (21) + νCr–O (10) + δ O–S–F ip (18) +ρCrO_2 op (12) + τ CrO_2 ip (11)
13		235	220	ρ CrO_2 (64) + τ CrO_2 ip (16)
14		155	148	ν Cr–O (32) + τ CrO_2 ip (20) + δ Cr–O_2 ip (11)
15		143	136	ν_s Cr–O (41)
16		98	93	ρ CrO_2 (36) + δ Cr–O_2 ip (35) + τSO_2 ip (12) + τw CrO_2 ip (11)
17		57	56	τ Cr–O–S–O ip (75) + δ Cr–O_2 ip (16)
B symmetry				
18	1233 sh	1374	1379	ν_a S=O (52) + ν_s SO_2 ip (30) + ν_a SO_2 op (12)
19	1209 vs	1149	1191	ν_a SO_2 ip (42) + ν_a S=O (40)
20	1026 s	1091	979	ν_s SO_2 op (47) + ν_a SO_2 ip (27) + ν_a Cr=O (14)
21	989 sh	895	946	ν_a Cr=O (95)
22	871 w	826	853	ν_s S–F (72)
23	734 m	657	684	δSO_2 ip (64) + ν Cr–O (24)
24	611 sh	557	578	ρ SO_2 ip (39) + ν Cr–O (18) + δ O–S–F op (15) + δSO_2 op (12)
25	514 w	506	506	wag SO_2 ip (59) + δ O–S–F op (17) + δSO_2 op (10)
26	450[d]	449	462	δO–S–F op (38) + δSO_2 op (18) + ρSO_2 ip (17) + δSO_2 op (11) + νCr–O (10)
27		361	355	wag CrO_2 (33) + δ O–S–F op (17) + ρ SO_2 ip (16) + νCr–O (14) + δSO_2 op (10)
28	330[d]	336	334	τSO_2 op (76) + δCrO_2 op (10)
29		257	240	wag CrO_2 (57)
30		214	204	τw CrO_2 (63) + δCrO_2 op (12)
31		132	128	ν Cr–O (32) + δCrO_2 op (12)
32		75	74	τ Cr–O–S–O op (73) + δCrO_2 op (18)
33		10	10	ν Cr–O (38) + τw CrO_2 op (15)

[a] This work
[b] DFT B3LYP/6-31G*
[c] From scaled quantum mechanics force field
[d] From Ref. [23]

with a PED contribution of 72 % by using 6-31G* basis set [12]. The four Cr–O symmetric stretching modes are calculated at 355, 274, 136, and 10 cm^{-1} and assigned according to the calculations. The last two bands are attributed to the Cr ← O antisymmetric and symmetric stretchings. Also, the two modes, CrO_2 in-phase and out-of-phase bending (O–Cr–O), are calculated at 148 and 128 cm^{-1}, respectively, and for this both modes were not assigned. The wagging, rocking, and twisting modes of the CrO_2 group are calculated strongly mixed with other modes. The first two modes are assigned as in the monodentate case (see Table 2.8), while the out-of-phase and in-phase twisting modes are calculated and assigned at 204 and 93 cm^{-1}, respectively.

In this compound, both structures are probably present in the solid phase because the comparison of each infrared spectrum (Fig. 2.3a, b) with the corresponding experimental ones is different between them, whereas a comparison between the average calculated infrared spectra, as explained before, demonstrates good correlation (Fig. 2.3c).

The average theoretical spectrum is as displaced in relation to the experimental ones, as shown in Fig. 2.4. In addition, the proposed theoretical Raman spectra for both structures of the compound are presented in Fig. 2.5.

2.6 Force Field

The harmonic force field and the force constants for chromyl fluorosulfate were calculated by using the scaling procedure of Pulay et al. [25, 26] with the

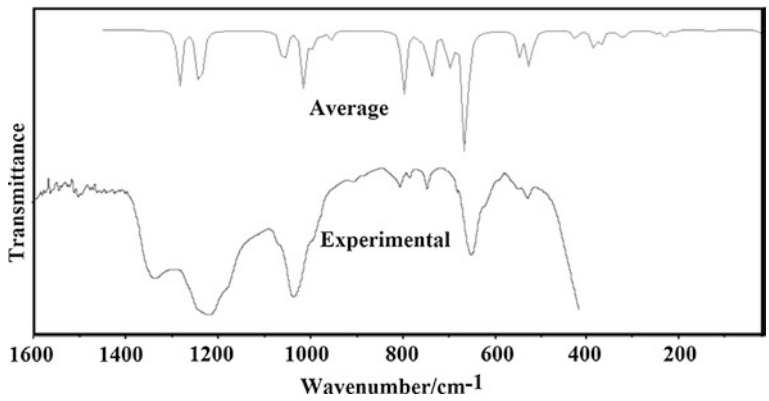

Fig. 2.4 Comparison between the infrared experimental spectrum of chromyl fluorosulfate with the calculated average infrared spectra for both structures from B3LYP/6–31G* wavenumbers and intensities using Lorentzian band shapes (for a population relation $C_2(1)$: $C_2(2)$ of 1: 1 for each structure). Reprinted from Journal of Molecular Structure, 981/1–3, A. Ben Altabef, S.A. Brandán, a new vibrational study of chromyl fluorosulfate, CrO2 (SO3F)2 by DFT calculations 146–152, copyright 2010, with permission from Elsevier

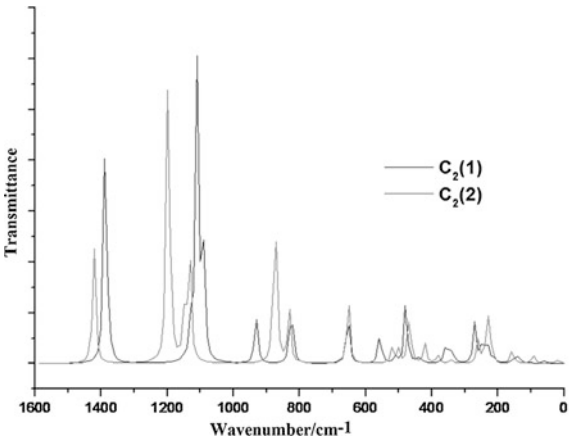

Fig. 2.5 Raman spectra for the theoretical $C_2(1)$ and $C_2(2)$ structures of chromyl fluorosulfate at B3LYP/6–31G* theory level. Reprinted from Journal of Molecular Structure, 981/1–3, A. Ben Altabef, S.A. Brandán, a new vibrational study of chromyl fluorosulfate, CrO2 (SO3F)2 by DFT calculations 146–152, copyright 2010, with permission from Elsevier

Table 2.12 Comparison of scaled internal force constants for chromyl fluorosulfate.

Force constant	B3LYP/6-31G*					
	[a]$CrO_2(SO_3F)_2$			[b]$CrO_2(NO_3)_2$		
	$C_2(1)$		$C_2(2)$	C_2		C_{3V}
	M	B	M	M	B	[a]SO_3F^-
f (S=O)	10.1	10.0	10.6			9.0
f (S–O)	6.4	8.6	4.7			
f (Cr=O)	6.6	6.6	8.8	6.55	6.53	
f (Cr–O)	2.8	1.3	3.7	6.09	1.44	
f (S–F)	5.2	5.2	4.8			4.0
f (O=S=O)	2.2	4.8	1.6			2.1
f (O=Cr=O)	2.4	2.3	2.1	2.53	1.66	
f (O–Cr–O)		0.8		0.80	0.93	
f (S–O–Cr)	1.8		0.4			
f (O–S–F)	2.0	2.6	1.7			1.6

Units are mdyn $Å^{-1}$ for stretching and stretching/stretching interaction and mdyn Å rad^{-2} for angle deformations

Abbreviations: *M* monodentate, *B* bidentate

[a] This work

[b] Ref. [12]

Reprinted from Journal of Molecular Structure, 981/1–3, A. Ben Altabef, S.A. Brandán, a new vibrational study of chromyl fluorosulfate, CrO2 (SO3F)2 by DFT calculations 146–152, copyright 2010, with permission from Elsevier

MOLVIB program [51, 52], as mentioned before. The calculated forces constants for both structures appear in Table 2.12.

In general, the calculated force constants for a bidentate coordination of the fluorosulfate groups in the $C_2(1)$ structure, with the B3LYP/6-31G* method, are approximately the same as the monodentate coordination of the same structure, with some variations in the *f*(S–O), *f*(Cr–O), *f*(O=S=O), and *f*(O−S−F) force

constants. The S–O and Cr–O stretching force constants change with the coordination mode of the fluorosulfate group, being the first one greater in the bidentate coordination (8.6 mdyn $Å^{-1}$) than in the monodentate coordination (6.4 mdyn $Å^{-1}$) because, in this case, there are two S–O stretchings in each fluorsulfate group (Fig. 1), while the Cr–O stretching force constant is greater in the monodentate coordination (2.8 mdyn $Å^{-1}$), as it was also observed in $CrO_2(NO_3)_2$ [12], because in the bidentate coordination there are four Cr–O stretchings. Also, the above reasons justify that the *f*(O=S=O) is greater in the bidentate coordination than the other coordination mode. On the other hand, the differences between the force constant values in the monodentate coordination of both structures are attributed to the geometrical parameters. Thus, the lower values of the force constants of O=S=O deformations in the $C_2(2)$ structure of chromyl fluorosulfate can be attributed to the higher values of the O=S=O angles (109.5°) in this structure than in the other ones (106.7°), while the lower *f*(O–S–F) force constant values in the $C_2(2)$ structure (1.7 mdyn Å rad^{-2}) are associated to the O–S-F angles values, because they are slightly higher (107.1°) in this structure than the corresponding values of the $C_2(1)$ structure (107.8°). The S=O stretchings force constants considering the two structures and coordination modes are near to the expected values reported by other compounds that contain SO_2 groups [49, 50]. The analysis of the force constants of the compound with the values for $CrO_2(NO_3)_2$ suggests that the coordination that better represents the fluorosulfate group in chromyl fluorosulfate is the bidentate ($C_2(1)$ structure), while when those values are compared with the SO_3F^- ion, the coordination that better represents the fluorosulfate group in chromyl fluorosulfate is the monodentate ($C_2(2)$ structure). This way, both coordination modes are possible in chromyl fluorosulfate.

2.7 Conclusions

The chromyl fluorosulfate molecule was synthesized and characterized by infrared spectroscopic techniques in the Nujol suspension.

The presence of both coordination modes was detected in the IR spectrum, and a complete assignment of the vibrational modes were accomplished.

The calculations suggest the existence of two molecular $C_2(1)$ and $C_2(2)$ structures for chromyl fluorosulfate, both of C_2 symmetries, which probably origin the different colorations observed by other authors in different preparations of the compound.

An SQM/B3LYP/6-31G* force field was obtained for both structures of chromyl fluorosulfate after adjusting the obtained theoretical force constants to minimize the difference between the observed and calculated wavenumbers.

The NBO and AIM analysis confirm the hexacoordination of the Cr atom in chromyl fluorosulfate.

Acknowledgments This work was subsidized with grants from CIUNT (Consejo de Investigaciones, Universidad Nacional de Tucumán), and CONICET (Consejo Nacional de Investigaciones Científicas y Técnicas, R. Argentina). The authors thank Prof. Tom Sundius for his permission to use MOLVIB.

References

1. E.L. Varetti, S.A. Brandán, A. Ben Altabef, Vib. Spectros. **5**, 219 (1993)
2. S.A. Brandán, A. Ben Altabef, E.L. Varetti, Spectrochim. Acta **51A**, 669 (1995)
3. S.A. Brandán, A. Ben Altabef, E.L. Varetti, J. Raman Spectrosc. **27**, 447 (1996)
4. S.A. Brandán, Estudio Espectroscópico de Compuestos Inorgánicos Derivados de Metales de Transición, Doctoral Thesis, National University of Tucumán, R. Argentina, 1997
5. S.A. Brandán, A. Ben Altabef, E.L. Varetti, Anales de la Asoc.Qca. Arg. **87**(1,2), 89 (1999)
6. O.E. Piro, E.L. Varetti, S.A. Brandán, A. Ben Altabef, J. Chem. Cryst. **33**, 57 (2003)
7. M. Fernández Gómez, A. Navarro, S.A. Brandán, C. Socolsky, A. Ben Altabef, E.L. Varetti, J. Mol. Struct. (Theochem) **626**, 101 (2003)
8. C. Socolsky, S.A. Brandán, A. Ben Altabef, E.L. Varetti, J. Mol Struct. (Theochem) **672**, 45 (2004)
9. M.L. Roldán, H. Lanús, S.A. Brandán, J.J. López, E.L. Varetti, A. Ben Altabef, J. Argent. Chem. Soc. **92**, 53 (2004)
10. M.L. Roldán, S.A. Brandán, E.L. Varetti, A. Ben Altabef, Z. Anorg, Allg. Chem. **632**, 2495 (2006)
11. S.A. Brandán, M.L. Roldán, C. Socolsky, A. Ben Altabef, Spectrochim. Acta, Part A **69**, 1027 (2008)
12. S.A. Brandán, C. Socolsky, A. Ben Altabef, Z. Anorg. Allg. Chem. **635**(3), 582 (2009)
13. S.A. Brandán, J. Mol. Struc. (Theochem) **908**, 19 (2009)
14. C.C. Addison, N. Logan, S.C. Wallwork, C.D. Garner, Q. Rev. Chem. **25**, 289 (1971)
15. C.C. Addison, N. Logan, Adv. Inorg. Chem. Radiochim. **6**, 71 (1964)
16. C.C. Addison, D. Sutton, Prog. Inorg. Chem. **8**, 195 (1967)
17. W.A. Guillory, M.L. Bernstein, J. Chem. Phys. **62**(3), 1059 (1975)
18. J. Laane, J.R. Ohlsen, Prog. Inorg. Chem. **27**, 465 (1980)
19. B. Lippert, C.J.L. Lock, B. Rosenberg, M. Zvagulis, Inorg. Chem. **16**, 1525 (1977)
20. C.J. Marsden, K. Hedberg, M.M. Ludwig, G.L. Gard, Inorg. Chem. **30**, 4761 (1991)
21. M. Lustig, G.H. Cady, Inorg. Chem. **1**(3), 714 (1962)
22. W.V. Rochat, G.L. Gard, Inorg. Chem. **1**(8), 158 (1969)
23. S.D. Brown, G.L. Gard, Inorg. Chem. **14**(9), 2273 (1975)
24. S. Bell, T.J. Dines, J. Phys. Chem. A **104**, 11403 (2000)
25. G. Rauhut, P. Pulay, J. Phys. Chem. **99**, 3093 (1995)
26. G. Rauhut, P. Pulay, J. Phys. Chem. **99**, 14572 (1995)
27. F. Kalincsák, G. Pongor, Spectrochim. Acta A **58**, 999 (2002)
28. A.E. Reed, L.A. Curtis, F. Weinhold, Chem. Rev. **88**(6), 899 (1988)
29. J.P. Foster, F. Weinhold, J. Am. Chem. Soc. **102**, 7211 (1980)
30. A.E. Reed, F. Weinhold, J. Chem. Phys. **83**, 1736 (1985)
31. E.D. Gledening, J.K. Badenhoop, A.D. Reed, J.E. Carpenter, F. Weinhold, *NBO 3.1* (Theoretical Chemistry Institute, University of Wisconsin, Madison, 1996)
32. R.F.W. Bader, *Atoms in Molecules, A Quantum Theory* (Oxford University Press, Oxford, 1990). ISBN: 0198558651
33. F. Biegler-Köning, J. Schönbohm, D. Bayles, AIM2000; a program to analyze and visualize atoms in molecules. J. Comput. Chem. **22**, 545 (2001)
34. A.B. Nielsen, A.J. Holder, *GaussView* (User′s Reference, Gaussian, Inc, Pittsburgh, 2000–2003)

35. M.J. Frisch, J.A. Pople, *Gaussian 03, Revision B.01* (Gaussian, Inc., Pittsburgh, 2003)
36. A.D. Becke, J. Chem. Phys. **98**, 5648 (1993)
37. C. Lee, W. Yang, R.G. Parr, Phys. Rev. B **37**, 785 (1988)
38. P.J. Perdew, Phys. Rev. B **33**, 8822 (1986)
39. P.J. Perdew, K. Burke, Y. Wang, Phys. Rev. B **54**, 16533 (1996)
40. A.W. Ross, M. Fink, R. Hilderbrandt, in *International Tables for Crystallography*, vol. C ed. by A.J.C. Wilson (Kluwer Academic Publishers, Dordrecht, Boston and London, p. 245, 404 1992)
41. Z. Žak, M. Kosička, Acta Cryst. **B34**, 38 (1978)
42. R.J. Gillespie (ed.), *Molecular Geometry* (Van Nostrand-Reinhold, London, 1972)
43. R.J. Gillespie, I. Bytheway, T.H. Tang, R.F.W. Bader, Inorg. Chem. **35**, 3954 (1996)
44. G.L. Sosa, N. Peruchena, R.H. Contreras, E.A. Castro, J. Mol. Struct. (Theochem) **401**, 77 409 (1997)
45. J. Goubeau, J.B. Milne, Canad. J. Chem. **45**, 2321 (1967)
46. R.J. Gillespie, R.A. Rothenbury, Can. J. Chem. **42**, 416 (1964)
47. R.J. Gillespie, E.A. Robinson, Can. J. Chem. **40**, 644 (1962)
48. A. Goypiron, J. De Villepin, A. Novak, J. Chim. Phys. **76**(3), 267 (1979)
49. H. Siebert, *Anwendungen der schwingungsspektroskopie in der Anorganische Chemie* (Springer, Berlin, 1966), p. 72
50. K. Nakamoto, *Infrared and Raman Spectra of Inorganic and Coordination Compounds*, 5th edn. (Wiley, New York 1997)
51. T. Sundius, J. Mol. Struct. **218**, 321 (1990)
52. T. Sundius, *MOLVIB: A Program for Harmonic Force Field Calculation*, QCPE Program No. 604 (1991)

http://www.springer.com/978-94-007-5762-2

A Structural and Vibrational Study of the Chromyl Chlorosulfate, Fluorosulfate, and Nitrate Compounds

Brandán, S.A.

2013, VII, 83 p. 13 illus., 3 illus. in color., Softcover
ISBN: 978-94-007-5762-2